

Strength and Sulfate Resistance of Mortar with Various Mortar Combinations

Wei Zhang¹, Rusheng Hao^{1,*}, Wenbo Wu¹, Yang Li¹ and Shiqiang Weng²

¹PowerChina Northwest Engineering Corporation Limited, Xi'an 710065, China

²Department of Civil and Environmental Engineering, Ruhr University, Bochum 44801, Germany

Received 1 January 2025; Accepted 8 April 2025

Abstract

The durability and safety of concrete structures exposed to environments such as saline soils or marine conditions are significantly reduced because of deterioration and degradation caused by sulfate ions. In order to improve the sulfate resistance of concrete, eight cementitious systems were prepared using two types of cement, the SY corrosion inhibitor, and different fly ash dosages. The influence of various raw materials on mortar strength was assessed via mortar strength tests, and the mortar specimens were subjected to long-term sulfate corrosion tests via the immersion method. The volume stability and strength retention of each cementitious system during sulfate corrosion were quantitatively evaluated on the basis of the expansion rate and corrosion resistance coefficient. The results indicate that, the mortar strength is enhanced by the addition of the SY corrosion inhibitor, whereas the P-O 42.5 cement exhibits a slightly greater strength than the P.MSR 42.5 cement. The expansion rate of the cementitious systems increases with immersion age, ranging from 0.015%–0.034% at 7 days to 0.101%–0.210% at 150 days. The expansion rate of the cementitious system is effectively reduced by using corrosion inhibitors or increasing the amount of fly ash. The corrosion resistance coefficient initially increases but then decreases with increasing immersion age, reaching a peak value at 60 days. Among the eight systems, the P.MSR 42.5 cement with 30% fly ash demonstrate the best performance in resisting sulfate attack, with a 150-day expansion rate of 0.101% and a corrosion resistance coefficient of 85.57%. This study provides valuable insights into optimizing concrete mix designs and improving the durability of structures exposed to sulfate attack.

Keywords: Cementitious system, Sulfate corrosion, Corrosion inhibitor, Expansion rate, Corrosion resistance coefficient

1. Introduction

Concrete is a heterogeneous and brittle material composed of cement, mineral admixtures, water, and aggregates. It is cost-effective and has excellent performance, making it widely used in various infrastructure constructions, such as roads, dams, and bridges. Currently, building structures are increasingly being developed in remote and complex areas, and concrete durability has become a growing concern. In engineering structures such as wind turbine foundations, long-span bridges, and underwater tunnels located in saline soils and marine environments [1], the presence of high sulfate contents poses a significant threat. Sulfate ions penetrate concrete through environmental water and react with cement hydration products, resulting in expansion, cracking, and spalling. These processes further lead to the loss of strength and stability in concrete structures, which can potentially cause premature structural failure before the intended service life is reached [2].

The primary cause of sulfate-induced degradation in concrete is the reaction between sulfate ions and cement hydration products within the concrete matrix, but aggregates are typically not involved in these reactions. Therefore, current research has focused predominantly on sulfate attack in cementitious materials [3]. Complex and long-term physical and chemical processes are often associated with sulfate corrosion, but no unified standard has been established to evaluate the resistance of cementitious systems to sulfate attack. This gap presents a challenge in enhancing the sulfate resistance of mortar and concrete

structures [4].

Numerous studies have also explored the physical and chemical mechanisms of sulfate corrosion in concrete [5–7], and research has shown that ordinary Portland cement cannot meet the durability requirements in high-sulfate environments [8]. Using high-volume fly ash to replace cement, modifying cement types, or incorporating sulfate-resistant corrosion inhibitors [9] can improve the sulfate resistance of cementitious systems [10]. However, these measures often neglect the negative impact on early-age mortar strength, and relying solely on isolated experimental tests might neglect long-term, comprehensive theoretical and experimental validation.

In this study, eight cementitious systems comprising two types of cement, varying fly ash dosages, and the SY corrosion inhibitor were investigated. Mortar strength tests, expansion rate tests, and corrosion resistance coefficient tests were performed to evaluate the influence of different material combinations on the strength and sulfate resistance of the systems. This study aims to provide valuable insights into improving concrete durability and optimizing cementitious material combinations to increase the service life of concrete structures.

2. State of the art

2.1 Network clustering

Sulfate attack on mortar can be classified into two main categories: physical crystallization damage and chemical corrosion [11–13]. Haynes et al. [14] described sulfate

*E-mail address: haorusheng@163.com

ISSN: 1791-2377 © 2025 School of Science, DUTH. All rights reserved.

doi:10.25103/jestr.182.01

crystallization damage as the recrystallization of salts within the pores of cement-based structures, where the generated crystals expand in volume and exert crystallization pressure on the pore structure, after which damage occurs. Biscaro et al. [15] reported that chemical corrosion damage occurs when sulfates react with cement hydration products to form expansive substances such as ettringite and gypsum, leading to cracks and even spalling on the surface of the hardened paste, ultimately damaging the concrete structure. However, in practical engineering, concrete degradation is driven by the combined effects of complex loading and corrosive solutions rather than a single form of physical or chemical erosion. Therefore, analyzing this phenomenon from a single perspective is insufficient.

Several methods have been developed to evaluate sulfate attack on mortars, including expansion rate tests, mass loss methods, and strength indices [16-18]. Mohr et al. [19] used mortar expansion rates to evaluate the sulfate resistance of composite cementitious systems. However, this method has a long testing period, and the specimens cannot be reused after testing, which can limit further analysis. Zhang et al. [20] evaluated the degree of corrosion in mortar immersed in sulfate solutions by measuring changes in specimen mass, but this method primarily reflects surface corrosion and cannot assess the internal structural damage of the mortar. Souza et al. [21] used the strength corrosion coefficient to intuitively reflect the impact of sulfates on the mechanical properties of cementitious materials. However, the specific causes of strength loss could not be identified, and early stages of corrosion could not be accurately demonstrated because early-stage strength loss was non-significant. Gao et al. [22] assessed the diffusion depth of sulfates in concrete via pore structure and permeability methods, but specialized equipment and personnel were needed, and the results needed to be interpreted in conjunction with other tests. Zhao et al. [23] microscopically analyzed changes in the mineral composition of mortar before and after sulfate corrosion via SEM and XRD, but high-quality test specimens were needed, and the degree of corrosion could not be quantified. These studies demonstrated that the use of a single evaluation index to assess the sulfate resistance of cementitious systems has limitations. Thus, evaluation approaches that can comprehensively combine multiple testing methods and practical conditions are necessary.

Studies on improving the sulfate resistance of mortar or concrete have focused primarily on reducing the content of tricalcium aluminate (C_3A) in cement, reinforcing fibers, and optimizing pore structures [24-26]. In terms of fiber reinforcement, Xu et al. [27] reported that concrete reinforced with steel fibers had higher strength and improved overall sulfate resistance; however, steel fibers are prone to corrosion in moist environments, and their durability requires further validation for long service life. Hu et al. [28] reported that basalt fibers have high durability and can mitigate the effect of sulfate corrosion on the bending strength of concrete, but dispersion tends to be uneven during construction, which can affect the integrity of concrete structures. Gan et al. [29] reported that polypropylene fibers in concrete can delay crack development and enhance resistance to sulfate corrosion, but strict control over the fiber dosage and mix ratio is needed to prevent any adverse effects on workability. Fares et al. [30] reported that high-performance concrete has far superior corrosion resistance compared with ordinary concrete, but its high cost restricts its large-scale application. In terms of pore structure optimization, Liu et al. [31] reported that sulfate-

resistant admixtures can improve the cement hydration process and increase the erosion resistance of mortar, but these additives are costly. Bai et al. [32] demonstrated that reducing the water-to-binder (W/B) ratio can lower the porosity of concrete, preventing the penetration of external sulfates and slowing the corrosion rate, but a lower W/B ratio can complicate construction. In terms of reducing the C_3A content, Tahwia et al. [33] reported that cement with a low C_3A content can effectively reduce the formation of ettringite and inhibit expansive damage to cementitious systems; however, such cements are expensive, which limits their widespread use. Ahmed et al. [34] showed that fly ash can reduce strength loss in mortar subjected to sulfate solutions, but excessive fly ash content decreases the early strength of mortar. Jagadisha et al. [35] reported that using slag to replace cement can reduce the amount of hydration products that react with sulfate ions, but this scheme increases the water demand of the mortar, which affects workability at high replacement levels.

The studies mentioned above have focused primarily on the mechanisms of sulfate attack on concrete and the enhancement of sulfate resistance in cementitious systems. On the one hand, these studies were based on isolated experimental results and lacked multidimensional experimental support. On the other hand, although cementitious systems are optimized, the focus of research has been on improving mortar resistance to sulfate attack, neglecting the impact on basic mechanical properties such as strength. In this study, eight cementitious systems consisting of two types of cement, fly ash, and SY corrosion inhibitor were developed by maintaining a fixed W/B ratio. Mortar strength tests were conducted to examine the influence of various materials on the strength of cementitious systems. Subsequently, expansion rate and corrosion resistance coefficient tests were performed to compare the impacts of different materials on the sulfate resistance of cementitious systems. This study aims to provide insights into optimizing cementitious material combinations of concrete and enhancing the sulfate resistance and

The remainder of this study is organized as follows: Section 3 describes the performance of the raw materials used, the mix proportions of the cementitious systems, and the experimental methods. Section 4 presents the influence of different material combinations on mortar strength and sulfate resistance. Analyses were performed via strength tests, expansion rate tests, and corrosion resistance coefficient tests. Section 5 summarizes the findings and presents the conclusions.

3. Methodology

3.1 Raw material

The types of cement used in this study were ordinary Portland cement (P·O 42.5) and sulfate-resistant Portland cement (P·MSR 42.5), both of which are 42.5 grade. The chemical compositions and mineral contents of both cements are presented in Table. 1, and their physical properties are presented in Table. 2. The sulfate resistance of both cements was assessed according to the gypsum method outlined in GB/T 749-2008. This method involves incorporating gypsum to increase the SO_3 content in the cement to 7.0%. The potential sulfate resistance of the cement mortar was then evaluated by measuring the expansion rate of the mortar specimens at the specified curing age. The 14-day linear

expansion rates of P·O 42.5 and P.MSR 42.5 were 0.036% and 0.019%, respectively. The sulfate resistance of P.MSR 42.5 was superior to that of P·O 42.5.

Class F II-level fly ash was used in this study, its water requirement ratio is 90% and strength activity index is 77.2%. Its chemical composition is presented in Table 1. The corrosion inhibitor used was SY, with an incorporation rate of 10%. The main manifestations of experimental sand are as follows: the China ISO standard sand is used for testing mortar strength, Sand with a particle size not exceeding 0.5mm is used to expansion rate testing and 0.5-1.0 mm intermediate sand was used for corrosion resistance coefficient testing.

3.2 Mix proportion

The W/B ratio for each mortar group was 0.5, and the sand-binder ratio was 2.5. The mix proportions and corresponding sample numbers are presented in Table. 3. The preparation

steps were as follows: first, water was added to the mixing bowl, and cement, fly ash, a corrosion inhibitor, and other materials were added. The mixture was stirred at low speed for 0.5 minutes. Then, sand was added, and the mixture was rapidly stirred for an additional 0.5 minutes.

The stirring was then stopped for 1.5 minutes, during which a spatula was used manually to scrape the mortar from the mixing blade, bowl wall, and bottom. Finally, the mixture was whisked at high speed for 1 minute before it was removed from the bowl.

The mortar mix proportions were named according to the following format: "cement type and dosage-fly ash dosage-corrosion inhibitor dosage." For example, PO70F20P10 represents a mixture with 70% P·O 42.5 cement, 20% fly ash, and 10% corrosion inhibitor, whereas PM80F20 represents a mixture with 70% P.MSR 42.5 cement and 20% fly ash.

Table 1. Chemical compositions and mineral composition ratios of cementitious materials

Type	Chemical composition mass ratio/%						Mineral composition mass ratio/%			
	SO ₃	MgO	CaO	SiO ₂	Fe ₂ O ₃	Al ₂ O ₃	C ₃ A	C ₂ S	C ₁ S	C ₄ AF
P·O 42.5	0.33	3.52	54.57	17.87	4.02	3.76	54.33	3.17	10.54	12.22
P.MSR 42.5	2.04	3.42	59.48	21.87	5.53	3.60	37.96	0.19	34.30	16.81
Fly ash	1.01	2.71	/	49.81	5.58	23.65	/	/	/	/

Table 2. Physical properties of the cement

Type	Density/g·cm ⁻³	Surface area/m ² ·kg ⁻¹	Standard consistence/%	Stability/mm
P·O 42.5	3.02	363	25.0	2.0
P.MSR 42.5	3.22	357	26.0	0.5

Table 3. Mix proportions of the adhesive sands (mass ratio)

Sample	Combination of cementitious materials	Cement	Fly ash	Preservative	Water	Sand
PO100	100%P·O 42.5	1	/	/	0.5	2.5
PO80-F20	80%P·O 42.5+20%Fly ash	0.8	0.2	/	0.5	2.5
PO70-F30	70%P·O 42.5+30%Fly ash	0.7	0.3	/	0.5	2.5
PO70-F20-P10	70%P·O 42.5+20%Fly ash+10%Preservative	0.7	0.2	0.1	0.5	2.5
PO60-F30-P10	60%P·O 42.5+30%Fly ash+10%Preservative	0.6	0.3	0.1	0.5	2.5
PM100	100%P.MSR 42.5	1	/	/	0.5	2.5
PM80-F20	80%P.MSR 42.5+20%Fly ash	0.8	0.2	/	0.5	2.5
PM70-F30	70%P.MSR 42.5+30%Fly ash	0.7	0.3	/	0.5	2.5

3.3 Test methods

The mortar strength evaluations were performed following the guidelines of GB/T 17671-2021. The mortar expansion rate testing was based on the Chinese standard CECS 207-2006 and the American standard ASTM C1202-2012. The test procedure was as follows: after the mortar was uniformly mixed, it was placed in a three-section mold (25 mm × 25 mm × 285 mm) equipped with measurement probes at both ends, with six specimens in each group. Following molding, the specimens were maintained at a temperature of 35±3 °C for 24 hours before being demolded. The specimens were subsequently placed in a saturated calcium hydroxide (Ca(OH)₂) solution for 3 days, after which the initial length (L_0) was measured. Furthermore, the specimens were submerged in a 5% Na₂SO₄ solution at 23±2 °C until the specified age was reached, after which the length (L_n) was measured. The expansion rate at different ages was calculated as:

$$L_p = \frac{L_n - L_0}{L} \times 100\% \quad (1)$$

where L_p is the expansion rate of the specimen after soaking for n days (%), L_n is the length of the specimen after

soaking for n days (mm), L_0 is the initial length of the specimen (mm), and L is the effective length of the specimen (mm).

The corrosion resistance coefficient of the mortar was calculated according to DL/T 5801-2019. The procedure for the test was as follows: initially, the thoroughly mixed mortar was loaded into a six-cavity mold measuring 10 mm × 10 mm × 60 mm. The mold with cores and casings was placed on a small pressure machine and subjected to a pressure of 7.8 MPa for 5 seconds. Following demolding, the surface of the mortar was smoothed using a scraper. Then, the samples were placed in a curing box and cured for 24±2 hours before demolding. After demolding, the specimens were transferred to water at 50±1 °C for 7 days. Finally, the specimens with identical mix proportions were divided into two groups: one was cured in 20 °C tap water, and the other was soaked in a 3% Na₂SO₄ solution. After the specimens had been soaked for the specified duration, they were removed and the surface moisture was wiped off before conducting the strength tests. The span of the specimens in the test was 50 mm, and the loading rate was 0.78 N/S. The corrosion resistance at different ages was calculated as:

$$K_n = \frac{R_{yz}}{R_{wn}} \times 100\% \quad (2)$$

where K_n is the corrosion resistance coefficient of the specimen after soaking for n days (%), R_{yn} is the strength of the specimen after soaking in 5% Na_2SO_4 solution for n days (MPa), and R_{wn} is the strength of the specimen after soaking in water for n days (MPa).

4. Result Analysis and Discussion

4.1 Mortar strength

The compressive strength and flexural strength of each cementitious system were measured according to the mortar strength testing method described in Section 3.3 (Fig. 1 and 2). The mortar strength of the P·O 42.5 cement was consistently greater than that of the P.MSR 42.5. A good explanation is that C_3A contributes significantly to early strength, and P.MSR 42.5 has a C_3A content of 0.19%, leading to a slower hydration reaction than P·O 42.5 does, resulting in lower strength. In the cementitious system composed of P·O 42.5, when the same amount of fly ash was added, the mortar strength with the corrosion inhibitor was slightly greater than that without the corrosion inhibitor. Therefore, the addition of a corrosion inhibitor can improve the mortar strength.

When fly ash was used to replace part of the cement, the strength of the mortar specimens decreased, and the mortar strength generally decreased with increasing fly ash content. The 28-day compressive strength of PO100 was 44.8 MPa, whereas for PO80-F20 (with 20% fly ash), it was 36.1 MPa, which was a 19.4% reduction compared with that of PO100; for PO70-F30 (with 30% fly ash), it decreased by 22.8%. However, as the curing period increased, the strength of the mortar with fly ash increased compared with that without fly ash. For example, the compressive strength ratios of PO80-F20 to PO100 at 7, 28, and 90 days were 79.1%, 80.6%, and 83.2%, respectively; the compressive strength ratios of PM70-F30 to PM100 at 7, 28, and 90 days were 63.0%, 71.7%, and 80.7%, respectively. A good reason is that fly ash mainly acts as a physical filler in the early hydration process of cementitious materials, and the volcanic ash effect is low, leading to lower early strength. However, as the curing period increased, fly ash gradually participated in the hydration reactions under the activation of $\text{Ca}(\text{OH})_2$, generating calcium silicate hydrate, such as C-S-H gel, thereby increasing the strength at later stages.

4.2 Expansion rate

The expansion rates of each mortar group at different curing ages are shown in Table. 4. The expansion rates of all the cementitious systems in the 5% Na_2SO_4 solution at 7 days were relatively small, ranging from 0.015% to 0.034%. However, as the curing period increased, the SO_4^{2-} ions in the solution reacted with C_3A , $\text{Ca}(\text{OH})_2$, C-S-H gel, and other components in the cementitious materials, generating expansive products such as gypsum ($\text{CaSO}_4 \cdot 2\text{H}_2\text{O}$) and ettringite (AFt) and increasing the expansion rates of the mortar specimens. The 150-day expansion rates of the various cementitious systems increased to 0.101%–0.210%. During the test period, the integrity of all the specimens remained high, and no chipping or edge degradation was

observed. Among all the cementitious systems, PO100 had the highest expansion rate, whereas PM70-F30 had the lowest expansion rate.

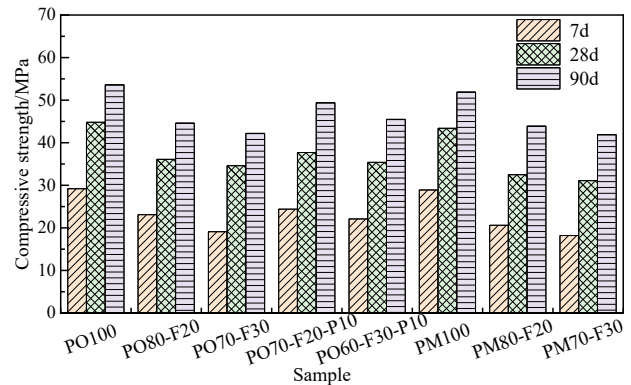


Fig. 1. Compressive strength of each mortar

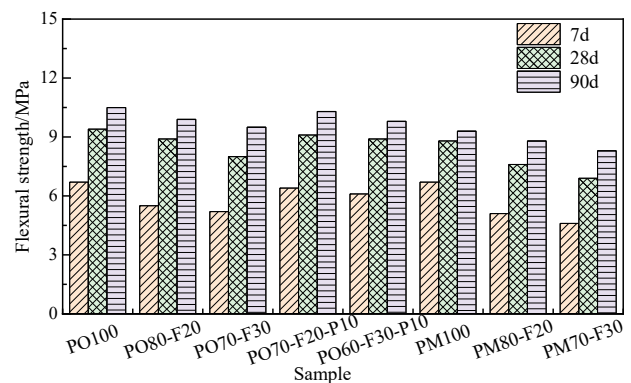


Fig. 2. Flexural strength of each mortar

In the five cementitious systems composed of P·O 42.5 cement, the expansion rates of the systems with only fly ash and those with fly ash and corrosion inhibitors were lower than those of PO100. Compared with those of PO100, the 150-day expansion rates of PO80-F20, PO70-F30, PO70-F20-P10, and PO60-F30-P10 decreased by 9.5%, 19.0%, 15.7%, and 23.3%, respectively. Thus, as the fly ash content increased, the expansion rate of the cementitious system decreased. The incorporation of fly ash might have not only reduced the C_3A content in the cementitious material but also underwent secondary hydration reactions with $\text{Ca}(\text{OH})_2$, forming a C-S-H gel. This situation reduced the amount of $\text{Ca}(\text{OH})_2$ that reacts with SO_4^{2-} in the soaking solution, thus decreasing the amount of AFt generated and lowering the expansion rate.

Additionally, the 150-day expansion rate of PM100 was 58.6% of that of PO100, the 150-day expansion rate of PM80-F20 was 57.9% of that of PO80-F20, and the 150-day expansion rate of PM70-F30 was 59.4% of that of PO70-F30. For the same fly ash content, the expansion rate of the P.MSR 42.5 cementitious system was much lower than that of P·O 42.5, indicating that P.MSR 42.5 cement had better sulfate resistance. On the one hand, the low C_3A content in P.MSR 42.5 likely reduced the likelihood of AFt formation; on the other hand, the higher C_4AF content in P.MSR 42.5 somewhat stabilized the reaction products with SO_4^{2-} , avoiding significant expansion, leading to a lower expansion rate in the Na_2SO_4 solution than in P·O 42.5.

Table 4. Expansion rate of each mortar sample at different times

Sample	Time/day									
	7	14	21	28	60	90	105	120	150	
PO100	0.034	0.073	0.095	0.104	0.155	0.174	0.183	0.193	0.210	
PO80-F20	0.029	0.065	0.075	0.097	0.133	0.157	0.170	0.175	0.190	
PO70-F30	0.019	0.043	0.059	0.085	0.117	0.134	0.143	0.151	0.170	
PO70-F20-P10	0.023	0.062	0.072	0.087	0.123	0.129	0.138	0.140	0.150	
PO60-F30-P10	0.021	0.041	0.055	0.079	0.108	0.122	0.126	0.129	0.131	
PM100	0.024	0.041	0.047	0.056	0.086	0.101	0.106	0.109	0.123	
PM80-F20	0.020	0.027	0.035	0.043	0.065	0.076	0.089	0.096	0.110	
PM70-F30	0.015	0.023	0.031	0.037	0.048	0.060	0.076	0.088	0.101	

4.3 Corrosion resistance coefficient

The strength of each mortar sample cured in water (R_{wn}) with age, obtained via the corrosion resistance coefficient test method for mortars described in Section 3.3, is shown in Fig. 3. The strength in the Na_2SO_4 solution (R_{yn}) is shown in Fig. 4, and the corrosion resistance coefficient changes with age are shown in Fig. 5. As can be seen from Fig. 3, with the increase of curing age, the strength of the mortar in each group increased. The 28-day strength of each cementitious system reached 83.8%-87.3% of the 150-day strength.

With increasing age, the corrosion resistance coefficient and R_{yn} of all the mortar groups initially increased but then decreased. The maximum values of R_{yn} and the corrosion resistance coefficient were reached at the 90-day curing age. The most significant decrease in R_{yn} and the corrosion resistance coefficient occurred between the 60-day and 90-day curing periods. Specifically, the corrosion resistance coefficient at 60 days was greater than 100%, but at 90 days, it was less than 100%. The reason for this trend was that in the initial stage of Na_2SO_4 erosion, the hydration reaction of the cementitious system was still ongoing, generating C-S-H to fill the pores, thus increasing the density of the mortar. Furthermore, SO_4^{2-} infiltrated via the tiny pores in the mortar specimens and reacted with hydration products such as $Ca(OH)_2$. Gypsum, ettringite, and sodium sulfate decahydrate ($Na_2SO_4 \cdot 10H_2O$) were generated, eventually filling the internal pores, increasing the compactness, and increasing the strength of the mortar. However, as the erosion period progressed, the hydration reactions gradually decreased, and the surfaces of the specimens noticeably eroded, which continuously increased the thickness of the eroded layer. The accumulation of corrosion products, along with the expansive nature of gypsum and ettringite, caused the pores inside the mortar to expand under stress. As microcracks formed, the mortar strength decreased.

In the P-O 42.5 cementitious systems with the same fly ash content, the corrosion resistance coefficient of the system with the corrosion inhibitor was greater than that of the system without the corrosion inhibitor (Fig. 4). When the fly ash content was 20%, the corrosion resistance coefficients of the system with the corrosion inhibitor at 90, 120, and 150 days were 88.74%, 86.59%, and 83.58%, respectively, demonstrating improvements of 7.49%, 6.49%, and 10.51%, respectively, compared with those of the system without the corrosion inhibitor. When the fly ash content was 30%, the improvements were 8.20%, 8.58%, and 10.62%, respectively. Thus, the addition of a corrosion inhibitor can increase the sulfate resistance of the cementitious system.

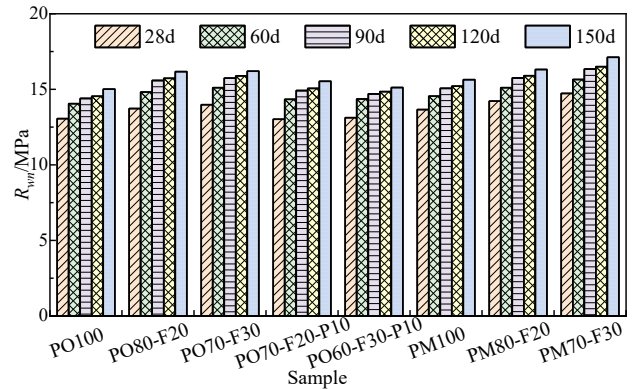


Fig. 3. Strength of mortar samples at different ages under water maintenance

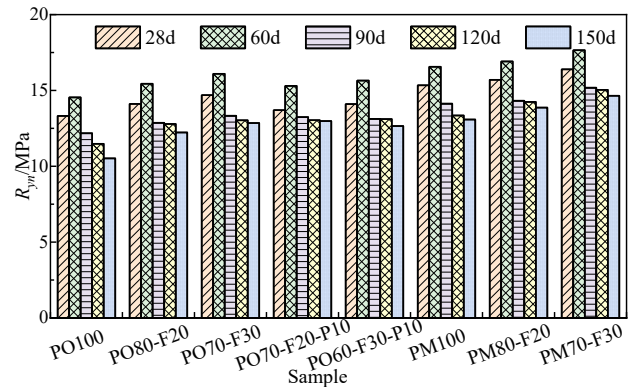


Fig. 4. Strength of mortar samples at different ages under Na_2SO_4 solution maintenance

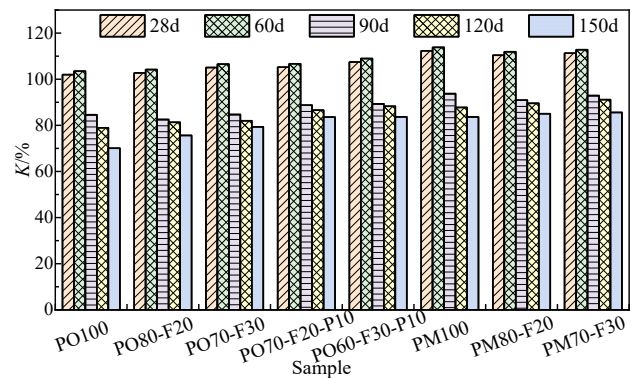


Fig. 5. K_r of the mortar samples at different ages

For systems with the same fly ash content, the corrosion resistance coefficient of the P.MSR 42.5 cementitious system was greater than that of the P-O 42.5 system. When the fly ash content was 0%, the 150-day corrosion resistance coefficient of PM100 was 1.19 times greater than that of PO100; when the fly ash content was 20%, the 150-day corrosion resistance coefficient of PM80-F20 was 1.12 times greater than that of PO80-F20; and when the fly ash content was 30%, the 150-day corrosion resistance coefficient of

PM70-F30 was 1.08 times greater than that of PO70-F30. Thus, the sulfate resistance of the P.MSR 42.5 cement was better than that of the P·O 42.5 cement.

In all cementitious systems, as the fly ash content increased, the corrosion resistance coefficient tended to increase. In the three cementitious systems composed of P·O 42.5 cement and fly ash, the 150-day corrosion resistance coefficient of PO100 was 70.09%. Compared with that of PO100, the coefficient of PO80-F20 was 75.63%, which was 7.90% greater than that of PO100. The coefficient of PO70-F30 was 80.70%, which is 13.17% greater than that of PO100. In the cementitious system composed of P·O 42.5 cement, fly ash, and a corrosion inhibitor, when the fly ash content increased from 20% to 30%, the corrosion resistance coefficient at 90 days improved by 0.65%, that at 120 days increased by 2.34%, and that at 150 days increased by 0.12%. In the cementitious system composed of P.MSR 42.5 cement and fly ash, when the fly ash content increased from 0% to 30%, the 120-day corrosion resistance coefficient increased from 87.77% to 91.15%, and the 150-day corrosion resistance coefficient increased from 83.63% to 85.57%. Fly ash improved the sulfate corrosion resistance of the cementitious system, and the improvement effect of fly ash on the cementitious system with P·O 42.5 cement was better than that with P.MSR 42.5 cement.

5. Conclusions

Mortar strength, expansion rate, and corrosion resistance coefficient tests were employed to investigate the effects of different material combinations on the strength and sulfate resistance of cementitious systems. The performances of various binder combinations were subsequently compared. The following conclusions could be drawn:

(1) As the fly ash content increases, the strength of cementitious systems generally decreases. For systems with the same fly ash content, the strength of P·O 42.5 cement-based sand is greater than that of P.MSR 42.5 cement-based sand. Additionally, a greater strength is exhibited by sand

containing the corrosion inhibitor than by that without the inhibitor.

(2) As the immersion age increases, the expansion rate of cementitious systems improves to varying extents. When fly ash and corrosion inhibitor are used to replace part of the cement, the expansion rate of the cementitious system is reduced.

(3) The corrosion resistance coefficient of cementitious systems increases with the addition of fly ash. For systems with the same fly ash content, the sulfate resistance of P.MSR 42.5 cement-based systems is superior to that of P·O 42.5 cement-based systems. Furthermore, with increasing immersion age in sulfate solution, the strength and corrosion resistance coefficient initially increase but then decrease, with the peak value observed at 60 days.

(4) For systems with the same fly ash content, the sulfate resistance performance follows the order of P.MSR 42.5+fly ash > P·O 42.5 cement+fly ash+SY corrosion inhibitor > P·O 42.5 cement+fly ash.

The effects of the fly ash content, corrosion inhibitor, and cement type on the sulfate resistance of cementitious systems were compared via sand expansion rate and corrosion resistance coefficient tests. The experimental results can provide theoretical and experimental references for enhancing the durability of concrete structures and constructing high-performance buildings. However, given that sulfate attack on concrete is a complex, long-term process involving physical and chemical interactions, only the corrosion resistance of specimens immersed in sulfate solution for 150 days was examined in this study. Longer-term experiments could be conducted in the future, and the microstructural evolution and performance degradation mechanisms during the corrosion process could be explored.

This is an Open Access article distributed under the terms of the Creative Commons Attribution License.



References

- [1] M.R. Sakr and M.T. Bassuoni. "Performance of concrete under accelerated physical salt attack and carbonation," *Cement Concrete Res.*, vol. 141, Mar. 2021, Art. no. 106324.
- [2] J. Guo, P. Liu, C. Wu, and K. wang, "Effect of dry-wet cycle periods on properties of concrete under sulfate attack," *Appl. Sci.*, vol. 11, no. 2, Jan. 2021, Art. no. 888.
- [3] M.M.A Elahi, *et al.* "Improving the sulfate attack resistance of concrete by using supplementary cementitious materials (SCMs): a review," *Constr. Build. Mater.*, vol. 281, Apr. 2021, Art. no. 122628.
- [4] F. Liu, Z. You, and R. Xiong, Y. Xu. "Effects of sodium sulfate attack on concrete incorporated with drying-wetting cycles," *Adv. Civ. Eng.*, vol. 2021, no. 1, Aug. 2021, Art. no. 5393504.
- [5] T. Yaowarat, *et al.* "Improved mechanistic performance of natural rubber latex modified pavement concretes in sulfate environments," *Int. J. Pavement Eng.*, vol. 25, no. 1, Jun. 2024, Art. no. 2353839.
- [6] Y. Liang and Z. Wang. "Investigation on performance degradation analysis method of offshore concrete structures under freeze-thaw and sulfate attack," *Ocean Eng.*, vol. 316, Jan. 2025, Art. no. 119935.
- [7] B. Xie, J. Yuan, and C. Jiang. "Experimental study on the mechanical properties of C30 molybdenum tailings concrete after high-temperature and sulfate corrosion," *Heliyon*, vol. 10, no. 22, Nov. 2024, Art. no. e40323.
- [8] J. Yang, Q. Ding, G. Zhang, D. Hou, M. Zhao, and J. Cao. "Effect of sulfate attack on the composition and micro-mechanical properties of C-A-S-H gel in cement-slag paste: A combined study of nanoindentation and SEM-EDS," *Constr. Build. Mater.*, vol. 345, Aug. 2022, Art. no. 128275.
- [9] S.U. Al-Dulajjan, M. Maslehuddin, M.M. Al-Zahrani, A.M. Sharif, M. Shameen, and M. Ibrahim. "Sulfate resistance of plain and blended cements exposed to varying concentrations of sodium sulfate," *Cemet Concrete Comp.*, vol. 25, no. 4, pp. 429-437, May. 2003.
- [10] G. Wang, *et al.* "Enhancing sulfate erosion resistance in ultra-high-performance concrete through mix design optimization using the modified andersen and andersen method," *Coating*, vol. 14, no. 3, Feb. 2024, Art. no. 274.
- [11] B. Tian and M.D. Cohen. "Does gypsum formation during sulfate attack on concrete lead to expansion?," *Cement Concrete Res.*, vol. 30, no. 1, pp. 117-123, Jan. 2000.
- [12] W. Bai, Y. Geng, C. Yuan, J. Guan, C. Xie, and L. Li. "Mesoscopic damage behavior of recycled aggregate concrete modified with metakaolin under the combined effects of freeze-thaw cycles and sulfate attack," *Arch. Civ. Mech. Eng.*, vol. 25, no. 2, Feb. 2025, Art. no. 91.
- [13] W. Xu, H. Liu, D. Qin, and S. Doh. "Study on the mechanical properties of desert sand concrete under dry-wet cycles with sulfate erosion," *Phys. Chem. Earth.*, vol. 138, Jun. 2025, Art. no. 103852.
- [14] H. Haynes, R. O'Neill, and P.K. Mehta. "Concrete deterioration from physical attack by salts," *Concr. Int.*, vol. 18, no. 1, pp. 63-68, Jan. 1996.
- [15] C. Biscaro, A. Martínez, A. Pérez, G. Xotta, C.M. López, and I. Carol. "'Onion-peel' cracking and spalling in coupled meso-

- mechanical analysis of External Sulfate Attack in concrete using zero-thickness interface elements,” *Constr. Build. Mater.*, vol. 455, Dec. 2024, Art. no. 139011.
- [16] L. Santillán, C. Zega, and E.F. Irassar. “Reactivity assessment of recycled concrete aggregates to sulfate attack,” *ACI Mater. J.*, vol. 121, no. 5, pp. 63-74, Sep. 2024.
- [17] O. Rokiah, *et al.* “Evaluation of the sulphate resistance of foamed concrete containing processed spent bleaching earth,” *Eur. J. Environ. Civ. Eng.*, vol. 26, no. 8, pp. 3632-3647, Jun. 2022.
- [18] N.A.M. Beltrame, A.V. Trisotto, R. Souto, J.A.N. Silva, B.C.G. Pereira, and R.A.M. Junior. “Effect of sulfate attack on geopolymer mortars at early ages of exposure,” *Mater. Struct.*, vol. 57, no. 10, Nov. 2024, Art. no. 239.
- [19] B.J. Mohr, M.S. Islam, and L. Bryant. “Long-term behavior of mortars experiencing delayed ettringite formation,” *Cement*, vol. 16, Jun. 2024, Art. no. 100104.
- [20] M. Zhang, D. Zou, S. Qin, X. Zhang, and T. Liu. “Decoupling chemical and physical sulfate attack on OPC and L. SAC concrete under wet-dry cycles,” *J. Build. Eng.*, vol. 99, Apr. 2025, Art. no. 111637.
- [21] D.J. Souza, M.H.F. Medeiros, and J. Hoppe Filho. “Evaluation of external sulfate attack (Na_2SO_4 and MgSO_4): Portland cement mortars containing siliceous supplementary cementitious materials,” *Rev. Ibracon. Estrut. Mater.*, vol. 13, no. 4, Sept. 2020, Art. no. e13403.
- [22] S. Gao, *et al.* “Analysis of performance evolution for the sulfate-eroded recycled concrete by using percolation method,” *Mater. Today Commun.*, vol. 44, Mar. 2025, Art. no. 111900.
- [23] G. Zhao, *et al.* “Degradation mechanisms of chloride contaminated cast-in-situ concrete partially exposed to magnesium-sulfate combined environment,” *KSCE J. Civ. Eng.*, vol. 27, no. 2, pp. 618-629, Feb. 2023.
- [24] A.B. Degefa and S. Park. “Phase diagrams for Portland cement-slag-fly ash ternary cements,” *Mater Struct*, vol 58, Jan. 2025, Art. no. 50.
- [25] Q. Yuan, J. Liu, C. Xu, F. Dang, H. Zhou, and L. Shi. “Experimental study and evaluation of bonding properties between fiber and cement matrix under sulfate attack,” *J. Build. Eng.*, vol. 76, Oct. 2023, Art. no. 107306.
- [26] D. Kanaan, A.M. Soliman, and A.R. Suleiman. “Zero-cement concrete resistance to external sulfate attack: a critical review and future needs”. *Sustain.*, vol. 14, no. 4, Feb. 2022, Art. no. 2078.
- [27] Q. Xu, X. Huang, and H. Wang. “Investigating the degradation process of steel fiber-reinforced concrete under sulfuric acid corrosion by combining laboratory tests and numerical modeling,” *Mater. Today Commun.*, vol 43, Feb. 2025, Art. no. 111598.
- [28] Y. Hu, *et al.* “The Improving Role of Basalt Fiber on the Sulfate-Chloride Multiple Induced Degradation of Cast-In-Situ Concrete,” *Materials*, vol. 17, no. 18, Sep. 2024, Art. no. 4454.
- [29] L. Gan, G. Liu, J. Liu, H. Zhang, X. Feng, and L. Li. “Three-dimensional microscale numerical simulation of fiber-reinforced concrete under sulfate freeze-thaw action,” *Case Stud. Constr. Mater.*, vol. 20, Jul. 2024, Art. no. e3308.
- [30] G. Fares, Y.M. Abbas, and M.I. Khan. “Deterioration mechanisms of Ultra-High-Performance concrete under various sulfuric acid and sulfate attack conditions,” *Arab. J. Sci. Eng.*, vol. 49, no. 10, pp. 14429-14445, May 2024.
- [31] K. Liu, Y. Sun, S. Shen, D. Sun, A. Wang, and Y. Wang. “Application of sulfate ion fixation in internal sulfate attack: The gel containing barium salt,” *Case Stud. Constr. Mater.*, vol. 20, Jul. 2024, Art. no. e02873.
- [32] M. Bai, Y. Lu, Z. Zhang, K. Cao, L. Cai, and H. Li. “Relationship between microscopic pore structure and strength of cement-based materials with low water-binder ratio under sulfate attack environment,”. *Sci. Adv. Mater.*, vol. 14, no. 4, pp. 725-735, Apr. 2022.
- [33] A.M. Tahwia, R.M. Fouda, M.A. Elrahman, and Osama. “Long-term performance of concrete made with different types of cement under severe sulfate exposure,” *Materials*, vol. 16, no. 1, Dec. 2022, Art. no. 111598.
- [34] A.D. Ahmed, A.A. Hammadi, M. Mohammed, and A.D. Jalal. “Response of fly ash based quarry dust cement mortar to magnesium sulphate attack,” *Ann. Chim. Sci. Mater.*, vol. 47, no. 2, pp. 67-73, Apr. 2023.
- [35] H.M. Jagadisha, S. Prashant, P. Pandit, S. G S, and R. Kamat. “Sulfate resistance of alkali-activated flyash-slag-lime concrete: comparative study of drying-wetting cycles and conventional exposure,” *Mater. Res. Express*, vol. 11, no. 10, Oct. 2024, Art. no. 111598.